Predicting photosynthetic structures using thermodynamics and machine learning

Callum Gray,[1] Samir Chitnavis,[1], Tamara Lucy Buja[1], Christopher D. P. Duffy[1*]

[1]Digital Environment Research Institute, Queen Mary University of London
Empire House, 67-75 New Road, London E1 1HH
[*]To whom correspondence should be addressed; E-mail: c.duffy@qmul.ac.uk

Oxygenic photosynthesis is responsible for nearly all biomass production on Earth, and may have been a prerequisite for the evolution of multicellular life. Life has evolved to perform photosynthesis under a wide range of illumination conditions, but with a common basic architecture of a light-harvesting antenna system coupled to a photochemical reaction centre. Using a general thermodynamic model of energy capture and diffusion in the antennae, coupled with a genetic algorithm to model their evolution, we reproduce qualitatively the antenna structures of multiple types of oxygenic photoautotrophs, including pigment composition, the linear absorption profile and the macrostructural topology, suggesting that the same simple physical principles underlie the development of distinct light-harvesting structures in various photosynthetic organisms. We finally apply our model to *extra-solar* light-environments and comment on the relative viability of both oxygenic and anoxygenic photosynthesis on exoplanets orbiting other types of stars.

Motivation: With the discovery of nearly 100 potentially-habitable exoplanets (*1*), the question of whether they do harbour life and what it might be like warrants serious consideration (*2*).

In which case, how do we meaningfully *hypothesize* (and not merely speculate) on the forms life might take in environments very different to Earth? Regardless of environment, evolution must be constrained by the laws of physics and chemistry; the question is then whether it is possible to develop a model that predicts the type of biological processes that will evolve under a given set of external conditions. Such a model must be broad, as it cannot presuppose any fine molecular detail, but must qualitatively capture the essential physics of basic biological functions.

However life may evolve, it will require an energy source, with the most obvious being the parent star. This implies that biospheres *in general* will be founded upon some form of photosynthesis. On Earth almost all of the primary production is via *oxygenic* photosynthesis, in which light is used to strip electrons from chlorophyll to produce energy and chemical reductants. The electrons are replenished by the splitting of water, producing our O_2 atmosphere, which may have been a prerequisite for the evolution of complex multicellular life (*3*).

The redox chemistry of water oxidation presents an energetic constraint, with photons of wavelength longer than about 700-750 nm insufficiently energetic to power the catalytic cycle (*4, 5*). While larger and warmer stars such as our Sun emit strongly in the visible range (400-700nm) and therefore provide a significant amount of usable light for oxygenic photosynthesis, cooler and smaller M-dwarf stars have limited emission in this range. At first glance, then, oxygenic photosynthesis would appear to be unfavourable around such stars (which include well known systems such as Trappist-1 (*6*) and Proxima Centauri (*7*)). This would appear to be a problem, since M-dwarfs are the most common star type in the universe (*8*) and have a high occurrence rate of Earth-like planets in their habitable zones (*9*).

However, recent experiments have shown that various oxygenic cyanobacteria, algae, moss and higher (vascular) plants are able to grow under simulated M-dwarf light (*10, 11*), though vascular plants show evidence of shade avoidance syndrome (*11*). While these are extremely

promising results, it does not necessarily follow that such organisms would *evolve* in such conditions. The response of vascular plants in particular suggests a stress response of an Earth organism subjected to unusual conditions, rather than evolution under such conditions.

While there is significant diversity in the microscopic structure of light-harvesting *antennae* between different kinds of organism which have evolved in different habitats, they all perform their function in a similar way: rather than absorbing light indiscriminately across the visible spectrum, they tend to absorb different wavelength bands selectively. Leaves are noticeably not black (*12*). Previous theoretical work has suggested that selective light-harvesting structures may have developed to balance capturing light against the metabolic cost of synthesising multiple pigment types (*12*), to absorb light preferentially at the maximum incident photon flux (*13, 14*), or to mitigate fluctuations in the light level in order to maintain the average power throughput of the antenna (*15*). In this work we consider a different potential organising principle: balancing photon flux capture with the thermodynamic and energetic limits on energy transfer.

Methodology: The act of light harvesting, intercepting photons over a large area and concentrating the resulting energy into a small reaction centre, reduces entropy ($\Delta S < 0$), which in itself is thermodynamically unfavourable (*16–18*). To counteract this, antennae are structured as "energy funnels" in which shorter wavelength (higher energy) pigments pass energy to longer wavelengths ones. In thermodynamic terms this is an enthalpy gradient ($\Delta H < 0$) which can over-compensate for the entropy reduction. Of course, this enthalpy gradient cannot be arbitrarily steep, since the antenna pigments should ideally absorb at wavelengths where there is a lot of incident flux. Moreover, different types of pigments should not be so different that they can no longer effectively exchange energy with each other. Lastly, the antenna should not be so large and complex that its creation and maintenance leaves little surplus energy for growth, reproduction, etc. (*12*)

Balancing these ideas, we construct a thermodynamic model of a light-harvesting antenna, allowing us to predict qualitatively how well-adjusted a given antenna structure is for a given light environment. This model calculates the overall electron output ν_e and efficiency ϕ of a given antenna for a given light input. We consider light-harvesting antennae which consist of an arbitrary number, n_b, of identical *branches* connected to a single reaction centre, with each branch composed of a number, n_s, of *subunits*, each with number, n_p, of identical photon-absorbing *pigments* (see Fig. 1A). The pigments that make up each subunit are chosen from a set of known photosynthetic pigments found in different niches on Earth, with their absorption spectra shown in Fig. 1B and further details in supplementary material. This is not an exhaustive list of organic pigments but covers most of the visible and far red regions of the spectrum. The antenna subunits absorb energy according to the incident photon flux, and the number, n_p and absorption spectra of their pigments. Energy transfer between subunits is assumed to be in thermodynamic *detailed balance*, with forward, k_f, and backward, k_b, transfer rates related by $k_f/k_b = \exp\left[-\beta\left(\Delta H_f - T\Delta S_f\right)\right]$. ΔH_f and ΔS_f are the enthalpy and entropy changes associated with energy transfer, which essentially depend on the relative energy and number, n_s, of the pigments in the two subunits. Lastly the reaction centre, in addition to its own pigments, also hosts a single *photochemical trap* which converts excitation energy into metabolically useful electrons. Since we are looking at *oxygenic* photoautotrophs, we assume that the the reaction centre pigment absorb at ~ 680 nm, though we relax this later. For details see (*19*) and the supplementary material. We purposely do not model microscopic details of the antenna subunits, nor consider any molecular physics beyond basic thermodynamics. The branch structure of the antenna should be interpreted topologically rather than as a physical supra-molecular structure. However, we did also consider the possibility of *inter-branch* transfer, which was found to have no impact whatsoever on antenna performance. The lateral and radial components of energy diffusion are orthogonal and energy trapping by the latter depends only on the latter.

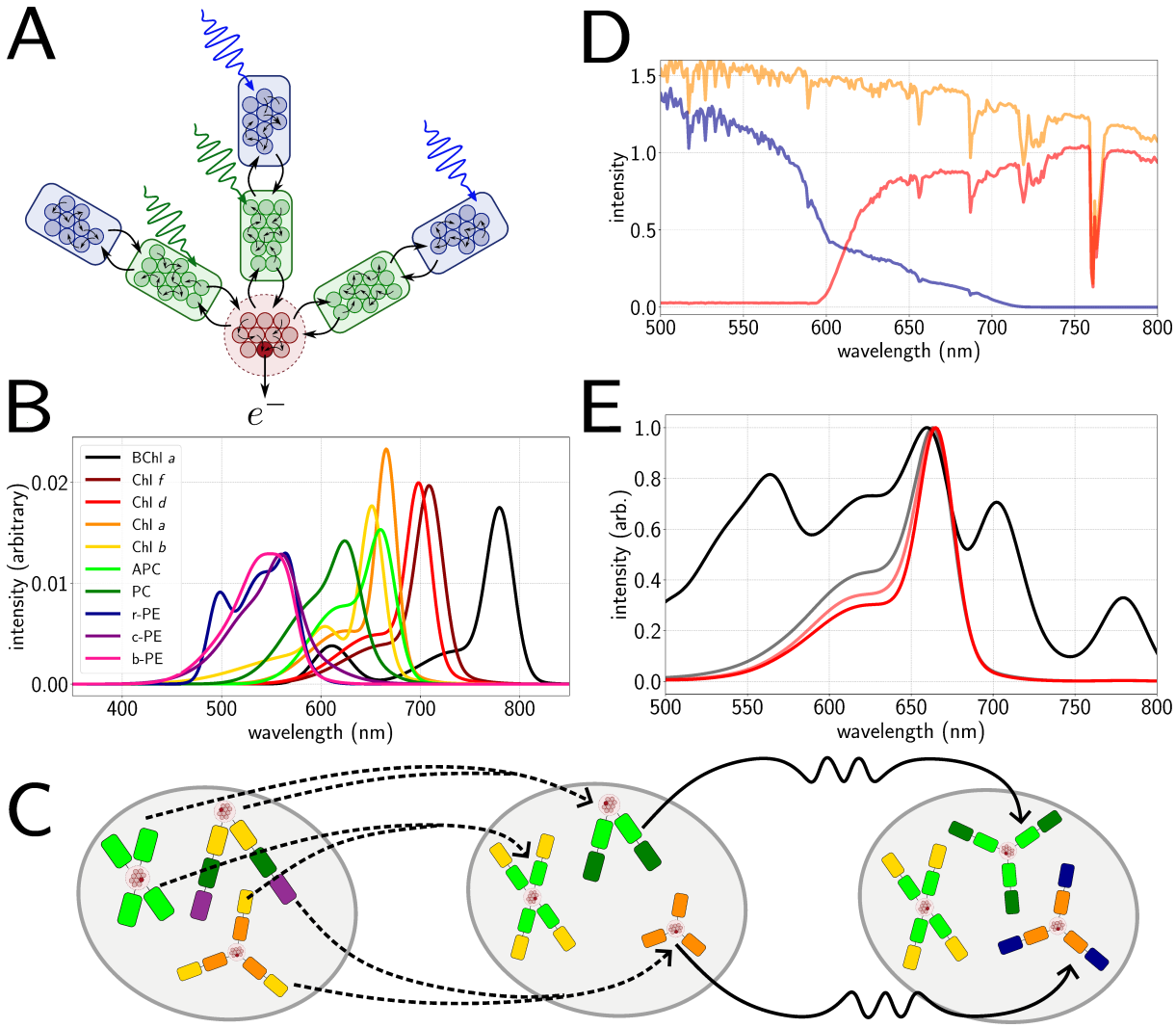

Figure 1: A.) Thermodynamic model of antenna. Rounded squares represent antenna subunits with the small circles representing pigments. Colour (green, blue) crudely represents absorption wavelength. Light is absorbed by each sub-unit and energy is transferred between them (black arrows), ending at the reaction centre (red) which traps (dark red) the energy and outputs electrons. B.) Absorption lineshapes of the available pigments for the genetic algorithm to choose from. Colour coding is repeated in Fig. 2 and throughout. C.) Genetic algorithm. Pairs of parents are selected (dashed lines) from the initial population to reproduce (left to middle), after which a mutation step is applied to members of the population at random (middle to right) to form the next generation. D.) Altering the light environment from full sunlight (yellow) to deep water (blue) or shaded (red) via filters. E.) Example of evolution of the average absorption spectrum from initial population (black) to a converged population (red) under red light illumination.

This model can then tell us qualitatively how well-suited a given light-harvesting structure is for a given light environment; for example, an antenna which absorbs preferentially in the blue at ~ 450 nm would be ill-suited to far red ($700 - 750$ nm) illumination. However, rather than simply producing well-adjusted structures by hand for specific light environments, which would be biased by our knowledge of light-harvesting structures on Earth, we pair the thermodynamic model with a machine learning algorithm which simulates evolutionary selection of particular structures.

This genetic algorithm treats the structural and absorption parameters of the antenna as a genome. We start with some initial population of *proto-antennae* and then simulate selection based on fitness, sexual reproduction (or "crossover"), and mutation through successive generations. Selection, crossover and mutation operators are defined (*20–22*) which act directly on the antenna structures to add or remove branches, increase or decrease branch length and change pigment composition as shown in Fig. 1C, drawing from the set of pigments shown in Fig. 1B (*23, 24*). Details of the implementation of the genetic algorithm can be found in the supplementary material. The selection operator requires a fitness function, which is a combination of electron output, ν_e, and a loosely defined "cost", χ: $F = \nu_e - \chi\left(\sum_{i=1}^{n_s} n_b n_p^i\right)$. χ represents the number of output electrons that have to be reinvested in maintaining the antenna itself. We should not over-interpret this as it could reflect abstract costs such as loss of internal space in the cell due to a massive antenna, the need for photo-protective mechanisms, the need to support non-photosynthetic tissues such as roots, etc. Through selection the initially diverse population of structures is optimised which can be visualized by the evolution of the antenna absorption spectrum as shown in Fig. 1E. Here an initially random population of different antenna subject to full sunlight gradually converges on something much more selective. By analysing population averages we can extract the pigment composition and antenna macrostructure of the converged population. We can also analyse absolute light-harvesting performance/feasibility in

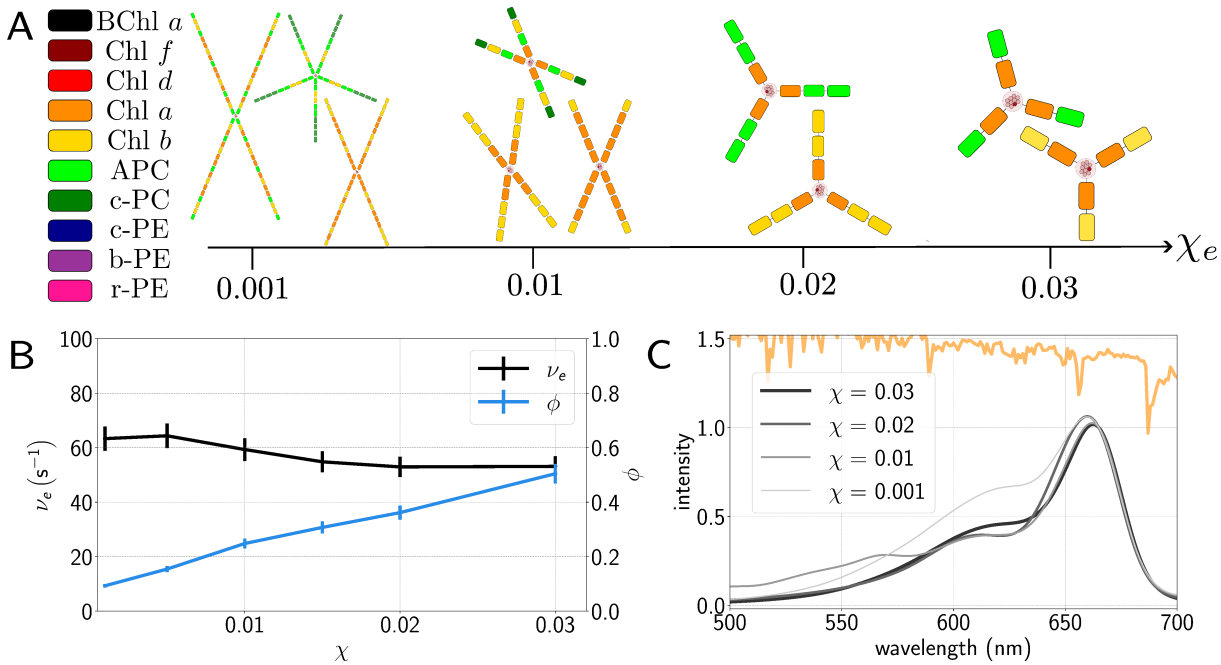

Figure 2: A.) Pictorial representation of example light-harvesting structures evolved under standard AM1.5 sunlight spectrum, as a function of the cost χ. Pigment blocks are colour-coded according to the left panel throughout the text. B.) Average electron output per second ν_e and antenna efficiency ϕ as a function of χ. C.) Average absorption spectrum of total population as a function of χ showing a longer tail and more featured spectrum as the cost decreases.

a given light-environment by looking at the electron output, ν_e, and quantum efficiency, ϕ_e, of the evolved antennae.

The *cost* of an antenna: Before we consider evolution in different light environments, we consider the cost parameter, χ. Fig. 2 summarizes a set of simulation for different values of χ for an *AM1.5* solar flux (*25*) (this roughly corresponds to full Sun in the southern states of the USA). In Fig. 2A we show the effect of cost on antenna macrostructure. A cost of $\chi = 0.001$ means 1 in every 1000 electrons produced by the reaction centre has to be reinvested in maintenance. This produces a heterogeneous population of antennae with 4-5 branches and a very large number of sub-units in each branch. The subunits tend to bind Chl *a*, Chl *b* and the phycobiliproteins allophycocyanin (APC) and c-phycocyanin (c-PC), with no obvious pattern.

Fig. 2B shows that these massive, poorly optimized antennae produce $\nu_e \sim 60$ electrons s^{-1} (the maximum possible is 100 s^{-1}) but with very low ($\phi \sim 0.1$) quantum efficiency. At low cost, there is no disadvantage to having a huge, inefficient antenna: so long as the electrons are delivered, efficiency is irrelevant. At cost of $\chi = 0.02 - 0.03$ (2-3 electrons reinvested for every 100 produced) the antennae are much smaller with less branches, though the electron output is not much decreased ($\nu_e \sim 55$ s^{-1}). Antennae consisting of Chl *a* and Chl *b* or Chl *a* and APC are selected and have much higher quantum efficiency ($\phi \sim 0.5$); at higher cost there is a serious disadvantage to having a huge inefficient antenna. The two selected types of antenna are qualitatively like PSII from higher plants (Chl *a* and Chl *b*) and PSII plus the phycobilisome core (Chl *a* and APC) from cyanobacteria. This can be seen in the absorption spectrum (Fig. 2C) which qualitatively looks like the red absorption band of plant PSII.

A sweep of χ for different light environments is presented in the Supplementary Material Figs. SM2–8, showing the similar pattern to Fig. 2. Low costs produce huge, inefficient and somewhat random antennae, while for $\chi > 0.03$ a stable population fails to evolve at all in some of the less ideal light-environments (see below). Even at higher costs, the predicted efficiencies are generally lower than $\phi_e > 0.8$ observed for *real* antenna systems, which we attribute to the deliberately crude nature of the underlying thermodynamic model. We therefore choose $\chi = 0.02$ to study different light environments in more detail.

Evolving antennae in different light: In Fig. 3 we consider additional light environments: red light such as found under leaf canopies (*26*), blue light as found under varying depths of clean water (*27*), and far red light (FRL) in which some species of cyanobacteria can survive by enriching their antenna and reaction centre with FRL-absorbing chlorophylls (an extreme survival response known a FaRLiP) (*5, 28, 29*). In each case our algorithm predicts structures using pigments commonly found in that environment as well as qualitatively reproducing important features of experimental absorption spectra.

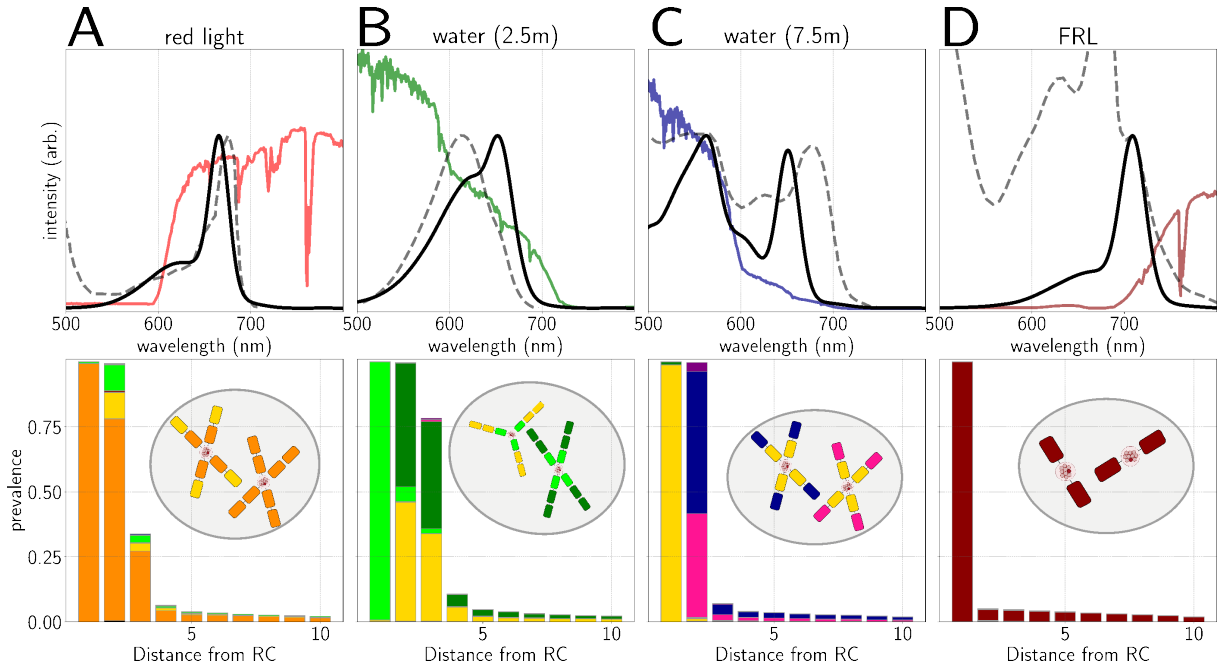

Figure 3: Top row: averaged absorption spectra of antennae (black lines) evolved in different light environments. Dashed lines are experimental absorption spectra for (A) PSII from vascular plant *Arabidopsis thaliana* (*30*), (B) Phycobilisome from filamental cyanobacterium *Arthrospira platensis* (*31*), (C) red macro-algae *Lithothamnion glaciale* (*32*) and (D) FarLiP cyanobacterium *Chroococcidiopsis thermalis* (*5*) plotted for comparison with the results of the genetic algorithm (solid lines); incident light spectra are plotted in colour. Bottom row: Pigment composition of antennae as a function of distance from the reaction centre (colour scheme as in Fig. 2), with example antennae shown in insets.

In red light (Fig. 3A) we see structures dominated by Chl *a*, with some Chl *b*, with a corresponding absorption peak very close to the red band of plant PSII. For water-attenuated light the flux becomes bluer with increasing depth (we considered 1-10 m depth (*27*)). We found two main regimes with representative results at 2.5 m and 7.5 m depth shown in Fig. 3B and 3C respectively. In shallower water (Fig. 3B) the evolved population is dominated by antennae containing mainly allophycocyanin (APC) and phycocyanin (PC) with absorption peaks at around 650 nm and 610 nm respectively. This lines up well with the absorption spectrum of the phycobilisome from a filamental cyanobacterium (dashed line) though the APC peak appears

only as a shoulder at 650 nm on the main PC peak at 610 nm.

In deeper water (Fig. 3C) we see instead two separated peaks at around 650nm and 560nm as the antennae reduce their PC content in favour of phycoerythrin (PE). This compares well with the absorption spectrum of the PE-enriched marine red alga (*32*). We note that some cyanobacteria also acclimate to bluer light by reducing their PC content in favour of PE via a process called group III complementary chromatic adaptation (CCA) (*33, 34*), although they do not stop producing PC entirely. In our model the subunits closest to the RC seem to prefer Chl *b* over APC, which we attribute to the longer tail of the Chl *b* lineshape giving a larger spectral overlap with PE. Spectroscopically, APC and Chl *b* are similar.

In FRL a functional antenna does not evolve (at higher cost; for lower cost values see Fig. SM7) due to the difficulty in transferring energy *uphill* to the 680 nm reaction centre. However, if we red-shift the reaction centre to ~ 720 nm (as in FarLiP cyanobacteria) we predict a small antenna composed of Chl *f*. The predicted absorption spectrum (Fig. 3D) lines up with the 720 nm absorption shoulder observed for the aforementioned FarLiP cyanobacteria. Even so, the overall electron output is an order of magnitude lower in FRL than in other light environments. This is consistent with the fact that even FarLiP cyanobacteria have restricted growth in FRL (*35*), FarLiP being a stress response rather than a long-term survival strategy.

Contingent evolution: So far all antenna have been assume to evolve *in situ* from a random population of *proto-antennae*. This may mean we miss potentially viable antenna configurations simply because there is no simple evolutionary path to them from a proto-antenna. In evolutionary terms we have neglected radiative adaptation, in which organisms adapt and spread beyond their initial environment. To investigate this, we take a population of "shallow water" type antennae composed of APC and PC and let them adapt to "deep water" conditions (see Fig 4A and SM9). As with the previous results our model predicts a PE-enriched antenna, similar to that found in deep water cyanobacteria and red algae. However, the APC antenna core is retained

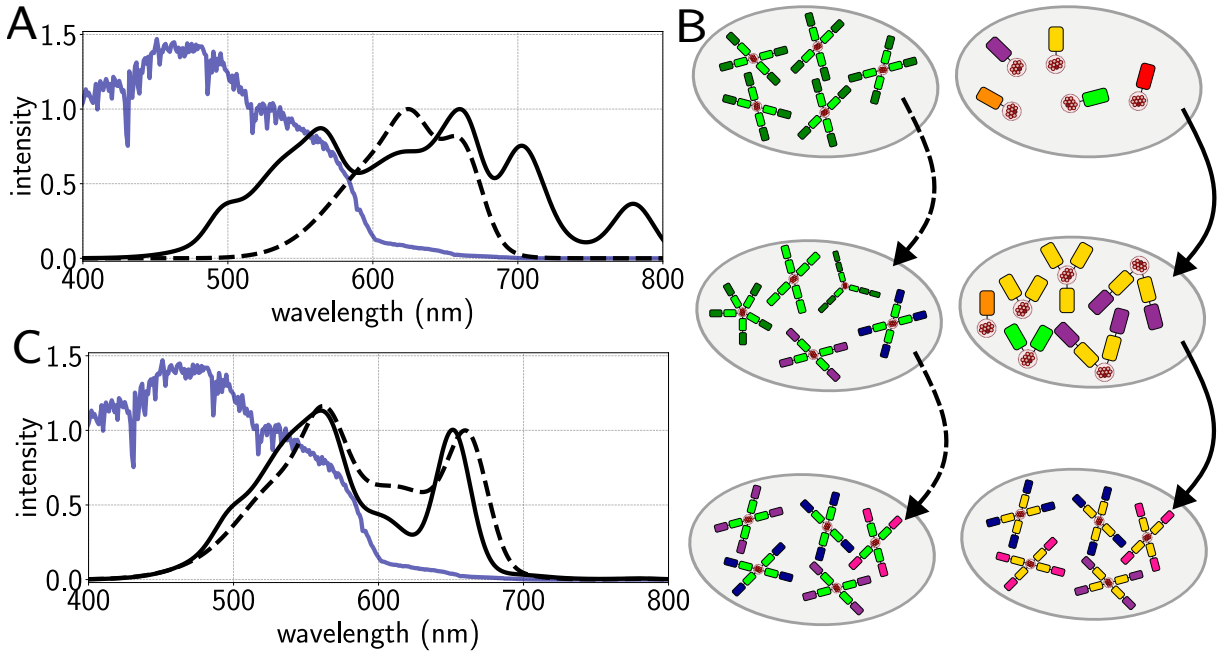

Figure 4: Comparison of contingent versus *in situ* evolution of antennae in deep water (10m). A.) Average initial absorption spectrum for *in situ* (solid line) and contingent (dashed line) populations. B.) Diagram showing evolution of contingent (left column, dashed arrows) and *in situ* (right column, solid arrows) populations evolving from top to bottom. C.) Averaged final absorption spectra for the *in situ* (solid line) and contingent (dashed line) populations.

(compared to Chl *b* for in situ evolution). The PC subunits are again substantially replaced by PE, similar to group III CCA in cyanobacteria, where PC levels can be dramatically reduced and PE increased in greener and bluer light (*34*). In terms of antenna performance, ν_e and ϕ_e are slightly reduced if we start out with a shallow water population rather than evolve from scratch, illustrating the history-dependence of evolutionary solutions (*36*).

Extra-solar light: Given that our model appears qualitatively robust, we apply it to fluxes typical of M- and K-dwarf stars. These are generated by taking PHOENIX model spectral fluxes for stellar temperatures of 2300 K and 3800 K respectively (*37*), and assuming an orbital distance that would allow for liquid water (*38*). Since recent research has noted the potential feasibility of *anoxygenic* photosynthesis arising around cooler stars (*39*), we compare our oxy-

genic model to a crude anoxygenic model with a reaction centre wavelength of 890 nm (*40–42*). In Fig. 5A we see that constrained by a 680 nm oxygenic reaction centre, a small antenna composed exclusively of Chl *a* evolves. The electron output is quite low ($\nu_e \sim 5$ s^{-1} (Fig. 5C) but this does not mean oxygenic photosynthesis would be ineffective. Several species of cyanobacteria have adapted to very low levels of illumination (*43*), and simulated M-dwarf light does not limit growth of cyanobacteria, even without the FaRLiP response (*11*).

For a 890 nm anoxygenic reaction centre, the model selects a much larger antenna composed of BChl *a* with an absorption peak of ~ 860 nm. The electron output is much higher ($\nu_e \sim 50$ nm), which casually suggests that anoxygenic may be a better evolutionary choice, though numerous other factors will be important. For warmer stars (Fig. 5B and 5C) an oxygenic photosystem, with an antenna composed of Chl *a* (and some Chl *b*), becomes more and more effective, with a sharp increase at $T = 2800$ K. For a K-dwarf star ($T = 3800$ K) the performance of the two types of photosystem are roughly equivalent. If there is any evolutionary preference, then it will be driven by factors other than light.

Concluding remarks: Our model, which is *necessarily* coarse-grained, when coupled with a sophisticated evolutionary algorithm, seems to predict (qualitatively) the various oxygenic light-harvesting structures that have evolved in various Earth niches. Applied to M-dwarf stars, it implies that oxygenic photosynthesis, utilising a Chl *a* antenna, may still evolve, though with reduced output relative to terrestrial organisms. This may limit oxygenic photosynthesis to simpler organisms that do not have to support massive amounts of non-photosynthetic tissue. We see this as a promising first step in producing a universal model of photosynthesis. It shows that we can, cautiously, hypothesize on the nature of biological processes beyond Earth. That said, like previous works (*12, 15*), we focus on light absorption and transfer, rather than the physics of energy conversion. The issue of oxygenic versus anoxygenic photosynthesis, or alternative FRL-variants of the former (*5, 28, 29, 44*), will require a more rigorous, though still

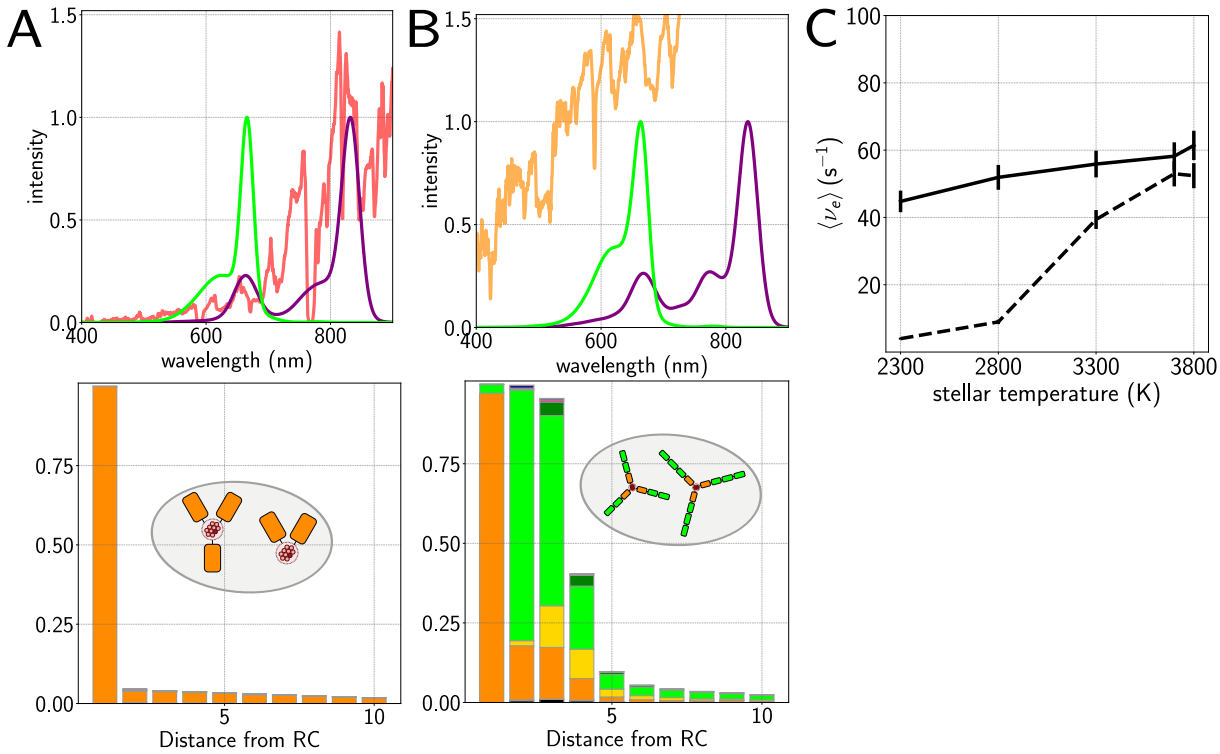

Figure 5: (A), (B) generated absorption spectra for oxygenic (green lines) and anoxygenic (purple lines) photosystems with pigment composition for the oxygenic antennae (bottom row) for stellar temperatures 2300K (M-dwarf, red line) (A) and 3800K (K-dwarf, orange line) (B). (C) Average electron output for oxygenic (dashed line) and anoxygenic (solid line) photosynthetic structures as a function of stellar temperature.

general, treatment of energy conversion in the reaction centre.

References and Notes

1. Habitable Worlds Catalogue, PHL@UPR Arecibo, https://phl.upr.edu/hwc. Updated: 2024-02-09.

2. C. McKay, *Proceedings of the National Academy of Sciences of the United States of America* **111** (2014).

3. D. B. Mills, D. E. Canfield, *BioEssays* **36**, 1145 (2014).

4. A. W. Rutherford, A. Osyczka, F. Rappaport, *FEBS letters* **586**, 603 (2012).

5. D. J. Nürnberg, *et al.*, *Science* **360**, 1210 (2018).

6. E. Agol, *et al.*, *The Planetary Science Journal* **2**, 1 (2021).

7. G. Anglada-Escudé, *et al.*, *nature* **536**, 437 (2016).

8. T. J. Henry, *et al.*, *The Astronomical Journal* **132**, 2360 (2006).

9. C. D. Dressing, D. Charbonneau, *The Astrophysical Journal* **807**, 45 (2015).

10. R. Claudi, *et al.*, *Life* **11**, 10 (2021).

11. M. Battistuzzi, *et al.*, *Life* **13**, 1641 (2023).

12. M. A. Marosvölgyi, H. J. van Gorkom, *Photosynthesis Research* **103**, 105 (2010).

13. N. Y. Kiang, *et al.*, *Astrobiology* **7**, 252 (2007).

14. N. Y. Kiang, J. Siefert, Govindjee, R. E. Blankenship, *Astrobiology* **7**, 222 (2007).

15. T. B. Arp, *et al.*, *Science* **368**, 1490 (2020).

16. R. C. Jennings, E. Engelmann, F. Garlaschi, A. P. Casazza, G. Zucchelli, *Biochimica et Biophysica Acta (BBA) - Bioenergetics* **1709**, 251 (2005).

17. K. Broess, *et al.*, *Biophysical Journal* **91**, 3776 (2006).

18. H. Dong, *et al.*, *European Physical Journal Special Topics* **230**, 867–871 (2021).

19. S. Chitnavis, *et al.*, *in review* (2024).

20. J. H. Holland, *Adaptation in Natural and Artificial Systems: An Introductory Analysis with Applications to Biology, Control, and Artificial Intelligence* (The MIT Press, 1992).

21. A. Eiben, J. Smith, *Introduction to Evolutionary Computing*, Natural Computing Series (Springer, Berlin, Heidelberg, 2015).

22. B. Alhijawi, A. Awajan, *Evolutionary Intelligence* **17**, 1245 (2024).

23. M. Taniguchi, H. Du, J. S. Lindsey, *Photochemistry and Photobiology* **94**, 277 (2018).

24. Kiang, Nancy, VPL Biological Pigments database, https://vplapps.astro.washington.edu/pigments.

25. C. A. Gueymard, *Solar Energy* **71**, 325 (2001).

26. M.-Y. Ho, F. Gan, G. Shen, C. Zhao, D. A. Bryant, *Photosynthesis Research* **131**, 173 (2017).

27. M. Stomp, J. Huisman, L. J. Stal, H. C. P. Matthijs, *The ISME Journal* **1**, 271 (2007).

28. F. Gan, G. Shen, D. A. Bryant, *Life* **5**, 4 (2015).

29. C. J. Gisriel, G. Shen, G. W. Brudvig, D. A. Bryant, *Journal of Biological Chemistry* **300** (2024).

30. E. Wientjes, H. van Amerongen, R. Croce, *Biochimica et Biophysica Acta (BBA) - Bioenergetics* **1827**, 420 (2013).

31. A. Fălămaș, S. A. Porav, V. Tosa, *Applied Sciences* **10**, 4045 (2020).

32. S. E. Voerman, A. Ruseckas, G. A. Turnbull, I. D. W. Samuel, H. L. Burdett, *BMC Biology* **20**, 291 (2022).

33. B. L. Montgomery, *Current Opinion in Plant Biology* **37**, 18 (2017).

34. D. M. Kehoe, A. Gutu, *Annual Review of Plant Biology* **57**, 127 (2006).

35. T.-S. Nien, D. A. Bryant, M.-Y. Ho, *Applied and Environmental Microbiology* **88**, e00562 (2022).

36. Z. D. Blount, C. Z. Borland, R. E. Lenski, *Proceedings of the National Academy of Sciences* **105**, 7899 (2008).

37. Husser, T.-O., *et al.*, *Astronomy and Astrophysics (A&A)* **553**, A6 (2013).

38. C. D. P. Duffy, *et al.*, *Monthly Notices of the Royal Astronomical Society* **526**, 2265 (2023).

39. L. F. Coelho, *et al.*, *Monthly Notices of the Royal Astronomical Society* **530**, 1363 (2024).

40. J. Deisenhofer, H. Michel, *Science* **245**, 1463 (1989).

41. M. M. Leonova, T. Yu. Fufina, L. G. Vasilieva, V. A. Shuvalov, *Biochemistry (Moscow)* **76**, 1465 (2011).

42. A. Niedringhaus, *et al.*, *Proceedings of the National Academy of Sciences* **115**, 3563 (2018).

43. M. Pierangelini, S. Stojkovic, P. T. Orr, J. Beardall, *Harmful Algae* **46**, 11 (2015).

44. M.-Y. Ho, N. T. Soulier, D. P. Canniffe, G. Shen, D. A. Bryant, *Current Opinion in Plant Biology* **37**, 24 (2017).

45. Acknowledgements, funding info, etc. go here!